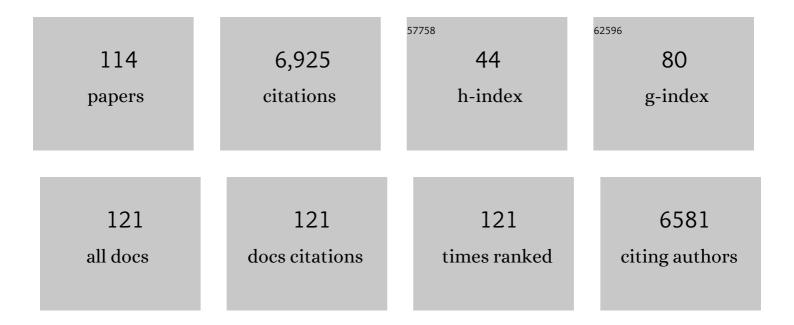
List of Publications by Year in descending order

Source: https://exaly.com/author-pdf/5043991/publications.pdf Version: 2024-02-01



#	Article	IF	CITATIONS
1	Selective photocatalytic reduction of CO2 to CO mediated by a [FeFe]-hydrogenase model with a 1,2-phenylene S-to-S bridge. Chinese Journal of Catalysis, 2021, 42, 310-319.	14.0	8
2	Interface-engineered silicon photocathodes with a NiCoP catalyst-modified TiO2 nanorod array outlayer for photoelectrochemical hydrogen production in alkaline solution. Journal of Power Sources, 2021, 484, 229272.	7.8	8
3	A silicon-based hybrid photocathode modified with an N ₅ -chelated nickel catalyst in a noble-metal-free biomimetic photoelectrochemical cell for solar-driven unbiased overall water splitting. Journal of Materials Chemistry A, 2021, 9, 12140-12151.	10.3	4
4	Efficient Iridium Catalysts for Formic Acid Dehydrogenation: Investigating the Electronic Effect on the Elementary β-Hydride Elimination and Hydrogen Formation Steps. Inorganic Chemistry, 2021, 60, 3410-3417.	4.0	16
5	Conjugated Linkers Improve the Photoelectrocatalytic H 2 â€Evolution Activity of Cobaloximeâ€Modified Silicon Photocathodes by Largely Suppressing Charge Recombination. Advanced Materials Interfaces, 2021, 8, 2100182.	3.7	3
6	Selective Electro-oxidation of Alcohols to the Corresponding Aldehydes in Aqueous Solution via Cu(III) Intermediates from CuO Nanorods. ACS Sustainable Chemistry and Engineering, 2021, 9, 11855-11861.	6.7	19
7	Boosting the performance of a silicon photocathode for photoelectrochemical hydrogen production by immobilization of a cobalt tetraazamacrocyclic catalyst. Journal of Materials Chemistry A, 2021, 9, 234-238.	10.3	10
8	Selective Hydrodeoxygenation of Guaiacol to Cyclohexanol Catalyzed by Nanoporous Nickel. Catalysis Letters, 2020, 150, 837-848.	2.6	17
9	Electrochemical Water Oxidation Catalyzed by N ₄ oordinate Copper Complexes with Different Backbones: Insight into the Structureâ€Activity Relationship of Copper Catalysts. ChemCatChem, 2020, 12, 1302-1306.	3.7	19
10	Boosting Electrocatalytic Water Oxidation by Creating Defects and Latticeâ€Oxygen Active Sites on Niâ€Fe Nanosheets. ChemSusChem, 2020, 13, 5067-5072.	6.8	12
11	A Dinuclear Copper Complex Featuring a Flexible Linker as Water Oxidation Catalyst with an Activity Far Superior to Its Mononuclear Counterpart. Inorganic Chemistry, 2020, 59, 5424-5432.	4.0	25
12	Spin-Controlled Charge-Recombination Pathways across the Inorganic/Organic Interface. Journal of the American Chemical Society, 2020, 142, 4723-4731.	13.7	25
13	Influence of Anchoring Groups on the Charge Transfer and Performance of p-Si/TiO ₂ /Cobaloxime Hybrid Photocathodes for Photoelectrochemical H ₂ Production. ACS Applied Materials & Interfaces, 2019, 11, 34010-34019.	8.0	13
14	Enhancing the Performance of Si-Based Photocathodes for Solar Hydrogen Production in Alkaline Solution by Facilely Intercalating a Sandwich N-Doped Carbon Nanolayer to the Interface of Si and TiO ₂ . ACS Applied Materials & Interfaces, 2019, 11, 19132-19140.	8.0	22
15	Fine-tuning the coordination atoms of copper redox mediators: an effective strategy for boosting the photovoltage of dye-sensitized solar cells. Journal of Materials Chemistry A, 2019, 7, 12808-12814.	10.3	12
16	Paired Electrocatalytic Oxygenation and Hydrogenation of Organic Substrates with Water as the Oxygen and Hydrogen Source. Angewandte Chemie, 2019, 131, 9253-9257.	2.0	47
17	Paired Electrocatalytic Oxygenation and Hydrogenation of Organic Substrates with Water as the Oxygen and Hydrogen Source. Angewandte Chemie - International Edition, 2019, 58, 9155-9159.	13.8	188
18	Charge transfer dynamics and catalytic performance of a covalently linked hybrid assembly comprising a functionalized cobalt tetraazamacrocyclic catalyst and CuInS ₂ /ZnS quantum dots for photochemical hydrogen production. Journal of Materials Chemistry A, 2019, 7, 27432-27440.	10.3	19

#	Article	IF	CITATIONS
19	Chemical Versatility of [FeFe]-Hydrogenase Models: Distinctive Activity of [μ-C6H4-1,2-(κ2-S)2][Fe2(CO)6] for Electrocatalytic CO2Reduction. ACS Catalysis, 2019, 9, 768-774.	11.2	21
20	Amorphous Ni(Fe)O H -coated nanocone arrays self-supported on stainless steel mesh as a promising oxygen-evolving anode for large scale water splitting. Journal of Power Sources, 2018, 389, 160-168.	7.8	20
21	Self-Supported Stainless Steel Nanocone Array Coated with a Layer of Ni–Fe Oxides/(Oxy)hydroxides as a Highly Active and Robust Electrode for Water Oxidation. ACS Applied Materials & Interfaces, 2018, 10, 8786-8796.	8.0	64
22	Atomic-level insight into super-efficient electrocatalytic oxygen evolution on iron and vanadium co-doped nickel (oxy)hydroxide. Nature Communications, 2018, 9, 2885.	12.8	669
23	Influence of the backbone of N ₅ -pentadentate ligands on the catalytic performance of Ni(<scp>ii</scp>) complexes for electrochemical water oxidation in neutral aqueous solutions. Chemical Communications, 2018, 54, 9019-9022.	4.1	28
24	Efficient and Stable Dye-Sensitized Solar Cells Based on a Tetradentate Copper(II/I) Redox Mediator. ACS Applied Materials & Interfaces, 2018, 10, 30409-30416.	8.0	31
25	Efficient dye-sensitized solar cells with [copper(6,6′-dimethyl-2,2′-bipyridine) ₂] ^{2+/1+} redox shuttle. RSC Advances, 2013 7, 4611-4615.	7, 3.6	48
26	Photocatalytic H ₂ production using a hybrid assembly of an [FeFe]-hydrogenase model and CdSe quantum dot linked through a thiolato-functionalized cyclodextrin. Faraday Discussions, 2017, 198, 197-209.	3.2	27
27	Highly active and durable electrocatalytic water oxidation by a NiB0.45/NiO core-shell heterostructured nanoparticulate film. Nano Energy, 2017, 38, 175-184.	16.0	71
28	Visible-light-absorbing semiconductor/molecular catalyst hybrid photoelectrodes for H ₂ or O ₂ evolution: recent advances and challenges. Sustainable Energy and Fuels, 2017, 1, 1641-1663.	4.9	68
29	Electrocatalytic water oxidation by copper(<scp>ii</scp>) complexes containing a tetra- or pentadentate amine-pyridine ligand. Chemical Communications, 2017, 53, 4374-4377.	4.1	71
30	Gas-templating of hierarchically structured Ni–Co–P for efficient electrocatalytic hydrogen evolution. Journal of Materials Chemistry A, 2017, 5, 7564-7570.	10.3	47
31	Competitive Hole Transfer from CdSe Quantum Dots to Thiol Ligands in CdSe-Cobaloxime Sensitized NiO Films Used as Photocathodes for H ₂ Evolution. ACS Energy Letters, 2017, 2, 2576-2580.	17.4	32
32	Improvement of Electrochemical Water Oxidation by Fineâ€Tuning the Structure of Tetradentate N ₄ Ligands of Molecular Copper Catalysts. ChemSusChem, 2017, 10, 4581-4588.	6.8	38
33	Low-cost solution-processed digenite Cu ₉ S ₅ counter electrode for dye-sensitized solar cells. RSC Advances, 2017, 7, 38452-38457.	3.6	6
34	Unraveling a Single-Step Simultaneous Two-Electron Transfer Process from Semiconductor to Molecular Catalyst in a CoPy/CdS Hybrid System for Photocatalytic H ₂ Evolution under Strong Alkaline Conditions. Journal of the American Chemical Society, 2016, 138, 10726-10729.	13.7	79
35	Effect of the S-to-S bridge on the redox properties and H ₂ activation performance of diiron complexes related to the [FeFe]-hydrogenase active site. Dalton Transactions, 2016, 45, 17687-17696.	3.3	19
36	Evident Enhancement of Photoelectrochemical Hydrogen Production by Electroless Deposition of M-B (M = Ni, Co) Catalysts on Silicon Nanowire Arrays. ACS Applied Materials & Interfaces, 2016, 8, 30143-30151.	8.0	40

#	Article	IF	CITATIONS
37	A Cuâ€Based Nanoparticulate Film as Superâ€Active and Robust Catalyst Surpasses Pt for Electrochemical H ₂ Production from Neutral and Weak Acidic Aqueous Solutions. Advanced Energy Materials, 2016, 6, 1502319.	19.5	36
38	Enhanced Photocatalytic Hydrogen Production by Adsorption of an [FeFe]â€Hydrogenase Subunit Mimic on Selfâ€Assembled Membranes. European Journal of Inorganic Chemistry, 2016, 2016, 554-560.	2.0	26
39	Electroless plated Ni–B films as highly active electrocatalysts for hydrogen production from water over a wide pH range. Nano Energy, 2016, 19, 98-107.	16.0	143
40	Effect of Bridgehead Steric Bulk on the Intramolecular C–H Heterolysis of [FeFe]-Hydrogenase Active Site Models Containing a P ₂ N ₂ Pendant Amine Ligand. Inorganic Chemistry, 2016, 55, 411-418.	4.0	17
41	Integration of organometallic complexes with semiconductors and other nanomaterials for photocatalytic H2 production. Coordination Chemistry Reviews, 2015, 287, 1-14.	18.8	140
42	The mechanism of hydrogen evolution in Cu(bztpen)-catalysed water reduction: a DFT study. Dalton Transactions, 2015, 44, 9736-9739.	3.3	32
43	Photochemical hydrogen production from water catalyzed by CdTe quantum dots/molecular cobalt catalyst hybrid systems. Chemical Communications, 2015, 51, 7008-7011.	4.1	44
44	CdSe quantum dots/molecular cobalt catalyst co-grafted open porous NiO film as a photocathode for visible light driven H ₂ evolution from neutral water. Journal of Materials Chemistry A, 2015, 3, 18852-18859.	10.3	72
45	Nickel Complex with Internal Bases as Efficient Molecular Catalyst for Photochemical H ₂ Production. ChemSusChem, 2014, 7, 2889-2897.	6.8	18
46	A super-efficient cobalt catalyst for electrochemical hydrogen production from neutral water with 80 mV overpotential. Energy and Environmental Science, 2014, 7, 329-334.	30.8	121
47	A Molecular Copper Catalyst for Electrochemical Water Reduction with a Large Hydrogenâ€Generation Rate Constant in Aqueous Solution. Angewandte Chemie - International Edition, 2014, 53, 13803-13807.	13.8	166
48	The influence of a S-to-S bridge in diiron dithiolate models on the oxidation reaction: a mimic of the Hairox state of [FeFe]-hydrogenases. Chemical Communications, 2014, 50, 9255-9258.	4.1	15
49	Highly efficient molecular nickel catalysts for electrochemical hydrogen production from neutral water. Chemical Communications, 2014, 50, 14153-14156.	4.1	65
50	Reactions of [FeFe]-hydrogenase models involving the formation of hydrides related to proton reduction and hydrogen oxidation. Dalton Transactions, 2013, 42, 12059.	3.3	104
51	Catalytic Activation of H ₂ under Mild Conditions by an [FeFe]-Hydrogenase Model via an Active μ-Hydride Species. Journal of the American Chemical Society, 2013, 135, 13688-13691.	13.7	107
52	Electrocatalytic hydrogen evolution from neutral water by molecular cobalt tripyridine–diamine complexes. Chemical Communications, 2013, 49, 9455.	4.1	91
53	Tetranuclear Iron Complexes Bearing Benzenetetrathiolate Bridges as Four-Electron Transformation Templates and Their Electrocatalytic Properties for Proton Reduction. Inorganic Chemistry, 2013, 52, 1798-1806.	4.0	31
54	Simple Nickelâ€Based Catalyst Systems Combined With Graphitic Carbon Nitride for Stable Photocatalytic Hydrogen Production in Water. ChemSusChem, 2012, 5, 2133-2138.	6.8	126

#	Article	IF	CITATIONS
55	Recent progress in electrochemical hydrogen production with earth-abundant metal complexes as catalysts. Energy and Environmental Science, 2012, 5, 6763.	30.8	474
56	Multielectronâ€Transfer Templates via Consecutive Twoâ€Electron Transformations: Iron–Sulfur Complexes Relevant to Biological Enzymes. Chemistry - A European Journal, 2012, 18, 13968-13973.	3.3	31
57	Photocatalytic H2 production in aqueous solution with host-guest inclusions formed by insertion of an FeFe-hydrogenase mimic and an organic dye into cyclodextrins. Energy and Environmental Science, 2012, 5, 8220.	30.8	114
58	Photocatalytic Water Reduction and Study of the Formation of Fe ^I Fe ^O Species in Diiron Catalyst Sytems. ChemSusChem, 2012, 5, 913-919.	6.8	42
59	Photochemical hydrogen production with molecular devices comprising a zinc porphyrin and a cobaloxime catalyst. Science China Chemistry, 2012, 55, 1274-1282.	8.2	16
60	Polymerization of rac-lactide catalyzed by group 4 metal complexes containing chiral N atoms. Polymer Bulletin, 2012, 68, 1789-1799.	3.3	6
61	Promoting Effect of Electrostatic Interaction between a Cobalt Catalyst and a Xanthene Dye on Visible-Light-Driven Electron Transfer and Hydrogen Production. Journal of Physical Chemistry C, 2011, 115, 15089-15096.	3.1	73
62	Approaches to efficient molecular catalyst systems for photochemical H2 production using [FeFe]-hydrogenase active site mimics. Dalton Transactions, 2011, 40, 12793.	3.3	116
63	Asymmetric oxidation of sulfides with H2O2 catalyzed by titanium complexes of Schiff bases bearing a dicumenyl salicylidenyl unit. Applied Organometallic Chemistry, 2011, 25, 325-330.	3.5	22
64	Assignment of the absolute configuration of dinuclear zirconium complexes containing two homochiral N atoms using TDDFT calculations of ECD. Chemical Physics Letters, 2011, 502, 266-270.	2.6	11
65	Effects of Additives on Water Solubilization Capacity and Intermicellar Interaction in Heptane/Hexanol/Tritonx-100/Water Microemulsion. Journal of Dispersion Science and Technology, 2011, 32, 415-423.	2.4	4
66	Synthesis of New Chiral Schiff Bases Containing Bromo- and Iodo-Functionalized Hydroxynaphthalene Frameworks. Synthetic Communications, 2011, 41, 1381-1393.	2.1	3
67	Homogeneous photocatalytic production of hydrogen from water by a bioinspired [Fe ₂ S ₂] catalyst with high turnover numbers. Dalton Transactions, 2010, 39, 1204-1206.	3.3	143
68	Photochemical H2 production with noble-metal-free molecular devices comprising a porphyrin photosensitizer and a cobaloxime catalyst. Chemical Communications, 2010, 46, 8806.	4.1	160
69	Highly enantioselective sulfoxidation with vanadium catalysts of Schiff bases derived from bromo- and iodo-functionalized hydroxynaphthaldehydes. Journal of Catalysis, 2010, 273, 177-181.	6.2	39
70	Hydrogen Production by Nobleâ€Metalâ€Free Molecular Catalysts and Related Nanomaterials. ChemSusChem, 2010, 3, 551-554.	6.8	75
71	Photocatalytic Hydrogen Production from Water by Noble-Metal-Free Molecular Catalyst Systems Containing Rose Bengal and the Cobaloximes of BF _{<i>x</i>} -Bridged Oxime Ligands. Journal of Physical Chemistry C, 2010, 114, 15868-15874.	3.1	151
72	Synthesis of Tri- and Disalicylaldehydes and Their Chiral Schiff Base Compounds. Synthetic Communications, 2010, 40, 1074-1081.	2.1	10

#	Article	IF	CITATIONS
73	Preparation and structures of enantiomeric dinuclear zirconium and hafnium complexes containing two homochiral N atoms, and their catalytic property for polymerization of rac-lactide. Dalton Transactions, 2010, 39, 4440.	3.3	39
74	Synthesis, protonation and electrochemical properties of trinuclear NiFe2 complexes Fe2(CO)6(1¼3-S)2[Ni(Ph2PCH2)2NR] (R=n-Bu, Ph) with an internal pendant nitrogen base as a proton relay. Inorganica Chimica Acta, 2009, 362, 372-376.	2.4	14
75	Protophilicity, electrochemical property, and desulfurization of diiron dithiolate complexes containing a functionalized C2 bridge with two vicinal basic sites. Polyhedron, 2009, 28, 1138-1144.	2.2	8
76	Synthesis and characterization of carboxy-functionalized diiron model complexes of [FeFe]-hydrogenases: Decarboxylation of Ph2PCH2COOH promoted by a diiron azadithiolate complex. Journal of Organometallic Chemistry, 2009, 694, 2309-2314.	1.8	25
77	Photochemical hydrogen production catalyzed by polypyridyl ruthenium–cobaloxime heterobinuclear complexes with different bridges. Journal of Organometallic Chemistry, 2009, 694, 2814-2819.	1.8	116
78	Light-driven hydrogen production catalysed by transition metal complexes in homogeneous systems. Dalton Transactions, 2009, , 6458.	3.3	241
79	Preparation, Facile Deprotonation, and Rapid H/D Exchange of the μ-Hydride Diiron Model Complexes of the [FeFe]-Hydrogenase Containing a Pendant Amine in a Chelating Diphosphine Ligand. Inorganic Chemistry, 2009, 48, 11551-11558.	4.0	84
80	Structures, protonation, and electrochemical properties of diiron dithiolate complexes containing pyridyl-phosphine ligands. Dalton Transactions, 2009, , 1919.	3.3	61
81	Asymmetric oxidation of sulfides with hydrogen peroxide catalyzed by a vanadium complex of a new chiral NOO-ligand. Catalysis Communications, 2009, 11, 294-297.	3.3	23
82	Influence of substituents in the salicylaldehydeâ€derived Schiff bases on vanadiumâ€catalyzed asymmetric oxidation of sulfides. Applied Organometallic Chemistry, 2008, 22, 253-257.	3.5	24
83	Synthesis and structure of a µâ€oxo diiron(III) complex with an <i>N</i> â€pyridylmethylâ€ <i>N</i> , <i>N</i> â€bis(4â€methylbenzimidazolâ€2â€yl)amine ligand and its catalytic property for hydrocarbon oxidation. Applied Organometallic Chemistry, 2008, 22, 573-576.	3.5	7
84	[FeFe]-Hydrogenase active site models with relatively low reduction potentials: Diiron dithiolate complexes containing rigid bridges. Journal of Inorganic Biochemistry, 2008, 102, 952-959.	3.5	16
85	An azadithiolate bridged Fe2S2 complex as active site model of FeFe-hydrogenase covalently linked to a Re(CO)3(bpy)(py) photosensitizer aiming for light-driven hydrogen production. Comptes Rendus Chimie, 2008, 11, 915-921.	0.5	30
86	Diiron dithiolate complexes containing intra-ligand NHâ< S hydrogen bonds: [FeFe] hydrogenase active site models for the electrochemical proton reduction of HOAc with low overpotential. Dalton Transactions, 2008, , 2400.	3.3	37
87	Noncovalent Assembly of a Metalloporphyrin and an Iron Hydrogenase Active-Site Model: Photo-Induced Electron Transfer and Hydrogen Generation. Journal of Physical Chemistry B, 2008, 112, 8198-8202.	2.6	150
88	A proton–hydride diiron complex with a base-containing diphosphine ligand relevant to the [FeFe]-hydrogenase active site. Chemical Communications, 2008, , 5800.	4.1	73
89	Supramolecular self-assembly of a [2Fe2S] complex with a hydrophilic phosphine ligand. CrystEngComm, 2008, 10, 267-269.	2.6	18
90	CO-Migration in the Ligand Substitution Process of the Chelating Diphosphite Diiron Complex (μ-pdt)[Fe(CO) ₃][Fe(CO){(EtO) ₂ PN(Me)P(OEt) ₂ }]. Inorganic Chemistry, 2008, 47, 6948-6955.	4.0	50

#	ARTICLE	IF	CITATIONS
91	Preparation, characterization and electrochemistry of an iron-only hydrogenase active site model covalently linked to a ruthenium tris(bipyridine) photosensitizer. Journal of Coordination Chemistry, 2008, 61, 1856-1861.	2.2	17
92	Visible Light-Driven Electron Transfer and Hydrogen Generation Catalyzed by Bioinspired [2Fe2S] Complexes. Inorganic Chemistry, 2008, 47, 2805-2810.	4.0	203
93	Synthesis of 3â€Arylâ€5â€tâ€butylsalicylaldehydes and their Chiral Schiff Base Compounds. Synthetic Communications, 2007, 37, 3815-3826.	2.1	7
94	Carbene–pyridine chelating 2Fe2S hydrogenase model complexes as highly active catalysts for the electrochemical reduction of protons from weak acid (HOAc). Dalton Transactions, 2007, , 1277-1283.	3.3	85
95	Protonation, electrochemical properties and molecular structures of halogen-functionalized diiron azadithiolate complexes related to the active site of iron-only hydrogenases. Dalton Transactions, 2007, , 3812.	3.3	60
96	Intermolecular Electron Transfer from Photogenerated Ru(bpy)3+to [2Fe2S] Model Complexes of the Iron-Only Hydrogenase Active Site. Inorganic Chemistry, 2007, 46, 3813-3815.	4.0	107
97	Phosphane and Phosphite Unsymmetrically Disubstituted Diiron Complexes Related to the Fe-Only Hydrogenase Active Site. European Journal of Inorganic Chemistry, 2007, 2007, 3718-3727.	2.0	32
98	Effect of Deprotonation of a Benzimidazolyl Ligand on the Redox Potential and the Structures of Mononuclear Ruthenium(II) Complexes. European Journal of Inorganic Chemistry, 2007, 2007, 4128-4131.	2.0	5
99	Synthesis, structures and electrochemical properties of hydroxyl- and pyridyl-functionalized diiron azadithiolate complexes. Polyhedron, 2007, 26, 904-910.	2.2	34
100	Preparation, structures and electrochemical property of phosphine substituted diiron azadithiolates relevant to the active site of Fe-only hydrogenases. Journal of Inorganic Biochemistry, 2007, 101, 506-513.	3.5	37
101	Influence of the built-in pyridinium salt on asymmetric epoxidation of substituted chromenes catalysed by chiral (pyrrolidine salen)Mn(III) complexes. Journal of Molecular Catalysis A, 2007, 270, 278-283.	4.8	10
102	An insight into the protonation property of a diiron azadithiolate complex pertinent to the active site of Fe-only hydrogenases. Chemical Communications, 2006, , 305-307.	4.1	73
103	Synthesis of chiral salen Mn(III) complexes covalently linked to Re(I)-based photosensitizers. Journal of Coordination Chemistry, 2006, 59, 475-484.	2.2	1
104	Asymmetric Oxidation of Sulfides Catalyzed by Vanadium(IV) Complexes of Dibromo- and Diiodo-Functionalized Chiral Schiff Bases. Chinese Journal of Catalysis, 2006, 27, 743-748.	14.0	22
105	Asymmetric epoxidation of styrene and chromenes catalysed by dimeric chiral (pyrrolidine) Tj ETQq1 1 0.784314	rgBT /Ove	erlack 10 Tf 5
106	An approach to water-soluble hydrogenase active site models: Synthesis and electrochemistry of diiron dithiolate complexes with 3,7-diacetyl-1,3,7-triaza-5-phosphabicyclo[3.3.1]nonane ligand(s). Journal of Organometallic Chemistry, 2006, 691, 5045-5051.	1.8	66
107	Asymmetric epoxidation of styrene and chromenes catalysed by chiral (salen)Mn(III) complexes with a pyrrolidine backbone. Journal of Catalysis, 2006, 237, 248-254.	6.2	30
108	Asymmetric oxidation of sulfides catalyzed by chiral (salen)Mn(III) complexes with a pyrrolidine backbone. Applied Organometallic Chemistry, 2006, 20, 830-834.	3.5	23

#	Article	IF	CITATIONS
109	Synthesis and property of a chiral salen Mn(III) complex covalently linked to an Ru(II) tris(bipyridyl) photosensitizer. Inorganic Chemistry Communication, 2005, 8, 606-609.	3.9	10

Influence of Tertiary Phosphanes on the Coordination Configurations and Electrochemical Properties of Iron Hydrogenase Model Complexes: Crystal Structures of [(μ-S2C3H6)Fe2(CO)6-nLn] (L =) Tj ETQq**0.0** 0 rgBT1‡@verlock

111	An Unusual Cyclization in a Bis(cysteinyl-S) Diiron Complex Related to the Active Site of Fe-Only Hydrogenases. Angewandte Chemie - International Edition, 2005, 44, 506-506.	13.8	0
112	Spectroscopic and crystallographic evidence for the N-protonated FelFel azadithiolate complex related to the active site of Fe-only hydrogenases. Chemical Communications, 2005, , 3221.	4.1	49
113	An Unusual Cyclization in a Bis(cysteinyl-S) Diiron Complex Related to the Active Site of Fe-Only Hydrogenases. Angewandte Chemie - International Edition, 2004, 43, 3571-3574.	13.8	26
114	Synthesis, Structures and Electrochemical Properties of Nitro- and Amino-Functionalized Diiron Azadithiolates as Active Site Models of Fe-Only Hydrogenases. Chemistry - A European Journal, 2004, 10, 4474-4479.	3.3	83